The heat budget of the earth's surface deduced from space

(*R.B. Smith; Version: March, 2010*)

1. Introduction

The objective of heat budget analysis is to estimate the processes adding and removing heat from the earth's surface. Heat budget analysis allows an understanding of the diurnal cycle of temperature, seasons, regional climate and the prediction of climate change. The equations for the surface heat budget are discussed in many textbooks and research papers. Stull (2004) gives a thorough review of boundary layer meteorology. Hartmann (1994) discusses the broader field of physical climatology. Barry (1992, Chapter 2) reviews the heat budget in mountainous regions. Liou (2002) gives a thorough review of atmospheric radiation. An example of using satellites to estimate heat budget terms is given in Schneider et al. (1996).

The governing equation for the surface heat budget is

$$MC_H \frac{d\overline{T}_S}{dt} = R_N - F_T \qquad (0)$$

The right hand side of (0) includes the rate at which energy is supplied to the earth's surface from short and long wave radiation (R_N) and the turbulent transport of heat to the atmosphere from the earth's surface (F_T). This turbulent transport includes, by convention, both the sensible heat and latent heat transport. The latent heat transport is the related to the evaporative cooling at the surface. The left hand side is the rate of change in heat storage in the soil layer. It is written using the mass of the soil being heated, its specific heat capacity and the time derivative of the surface temperature. Expressed in words, (0) states that if the net radiation input and turbulent heat flux output are not equal, the soil must be warming or cooling with time to store the heat excess or deficit. This equation simply expresses conservation of energy.

Under many circumstances, the two terms on the RHS nearly cancel. Consider a full year, where the temperature (and therefore the stored soil heat) is the same at the beginning and end of the period. In that case the average net radiation and average turbulent heat flux must cancel. This cancellation may also be found over a full 24-hour period. In some terrains, the cancellation may even occur at an instant. With loose granular soil or a dense vegetated canopy, the storage term will be small. Storage terms are especially important in cities and in rocky areas where heat can conduct into and out of a solid material. Storage is also important in bodies of water where turbulent motion can transport heat away from the surface. Heat can also be "stored" by melting ice.

In situations with negligible heat storage, the terms on the right hand side of (0) must quickly adjust themselves to maintain heat balance. This can be done by changing the temperature of the surface or the air, changing the evaporation rate, or by changing the

intensity of the turbulence. Everyday experience confirms this idea. When the sun rises in the morning (increasing the net radiation), the ground surface warms quickly, followed by increases in air temperature, evaporation rate and air turbulence.

The study of the surface heat budget has mostly developed using flux towers. A flux tower is a short tower with rapid response instruments measuring air temperature, humidity, vertical air speed and the long and short radiation component. The eddy correlation method is used to determine the sensible and latent heat fluxes. A few temperature sensors in the ground can give the heat storage.

In the sections below, we describe how to estimate the terms in (0) from satellite data. This method will never be as accurate as *in situ* measurements from flux towers, but it allows spatial analysis.

2. Solar Radiation (VIS and SWIR)

a. Simple equations

The incoming solar radiation on a clear day can be estimated from the following formulae. The strength of the direct solar beam falling on a level surface at the top of the atmosphere (TOA) is given by

$$Direct_{TOA} = S \cdot \cos(\theta_S) \qquad (1)$$

where S is the Solar Constant and θ_S is the solar zenith angle. The units in (1) are W/m2. According to (1), as the solar zenith angle increases, the radiant energy received per unit area decreases. At the earth's surface, the strength of the incident solar beam is

$$Direct = S \cdot T_0^m \cdot \cos(\phi) \qquad (2)$$

The middle factor in (2) represents the absorption and scattering of light out of the direct beam by the atmosphere. T_0 is the transmissivity of the full atmosphere to a vertical beam of solar radiation. Terrain altitude and sun angle are accounted for through the exponent

$$m = \frac{\exp(-z / H_L)}{\cos(\theta_s)} \qquad (3)$$

where z is the altitude in meters and HL is the scale height for absorbers and scatterers. For the present purposes we choose T_0=0.7 and $H_L = 4000m$. As the solar zenith angle increases, the exponent m increases due to the longer path length of the sun's rays in the atmosphere. As altitude increases, m approaches zero and the effects of absorption and scattering on the direct beam diminish.

The last factor in (2) represents the influence of terrain slope and aspect. For example, south facing slopes will receive more solar energy per unit area than north facing slopes in the northern hemisphere. The parameter (ϕ) is the angle between the sun's beam and the surface normal vector. This angle can be written using the slope, aspect, solar zenith angle, and solar azimuth angle (Law and Nichol, 2004).

$$\cos\phi = \cos(E)\cos(\theta_S) + \sin(E)\sin(\theta_S)\cos(A_0 - A_s) \qquad (4)$$

Where: E is the slope (in radians)
θ_S is the solar zenith angle (90 degrees minus the solar elevation angle)
A_0 is the solar azimuth angle
A_s is the surface aspect angle

Note that for a level surface (i.e. E=0), (4) reduces to $\cos(\phi) = \cos(\theta_S)$.

The diffuse radiation from the sun (i.e. skylight) could be approximately represented by

$$Diffuse = f \cdot S \cdot \cos(\theta_S)\exp(-z / H_L) \qquad (5)$$

where f is the maximum fraction of the sun's radiation that is scattered downward. For example, we choose f = 0.1 to describe a 10% scattering. As the diffuse radiation is nearly isotropic, we neglect terrain slope effects in (5). At high altitudes ($z \to \infty$), the diffuse radiation vanishes and the sky appears black.

The total solar irradiance at the earth's surface is the sum of the direct and diffuse parts.

$$TotalSolar = Max[Direct, 0] + Diffuse \qquad (6)$$

The "max" operator removes the negative values in Direct (2) that can occur in very steep terrain (i.e. terrain in shadow). Our formulation does not account for shadows that are "cast" by high peaks onto level terrain. Neither does our formulation account for the reduction of diffuse radiation in deep valleys caused by limited sky view.

In (1) and (2), S is the solar constant. The average value over a year is $\bar{S} = 1366 Wm^{-2}$, while the actual value changes through the year due to the ellipticity of the earth's orbit. S varies from 1412W/m2 at the January perihelion to 1321W/m2 at the July aphelion. It can be computed from $S = \bar{S} / d^2$ where d is the earth-sun distance expressed in astronomical units (AU). When working with individual spectral bands, the sun's radiation can be written

$$S_\lambda = ESUN_\lambda / d^2 \qquad (7)$$

where $ESUN_\lambda$ is the solar irradiance for a particular spectral band, at d =1.

b. Solar Analyst

Another approach is to use the Solar Analyst software to compute the incident solar radiation on complex terrain (Solar Analysts 1.0 User Manual). While it uses many of the above equations, it is more sophisticated than the methods described above. It takes into account terrain slope and aspect, and correctly accounts for shadows and reduced diffuse radiation in deep valleys. It prescribes an attenuation of the solar beam by the atmosphere that increases for larger solar zenith angles. It also takes into account the reduced attenuation (i.e. stronger beam) reaching higher elevations. It produces estimates of the direct beam (SAD) and the total incident solar radiation (SAT) including diffuse radiation (i.e. skylight). It does not treat individual spectral bands, only the total radiation in the solar spectrum.

c. Reflectance and Albedo

Using the satellite-derived radiances (I_λ), the top-of-atmosphere reflectance in each band can be computed from

$$\rho_\lambda = \frac{\pi I_\lambda}{S_\lambda} = \frac{\pi I_\lambda d^2}{ESUN_\lambda \cdot \cos(\theta_S)} \tag{8}$$

(Landsat 7 Users Handbook – Chapter 11). In (8), the factor π arises from our assumption of Lambertian reflection. This formula takes no account of atmospheric effects or non-level terrain surfaces.

For heat budget calculations, we define the albedo (a) as the average reflectance over the sun's spectrum. The albedo is computed by averaging the measured band reflectances. The simplest method is an unweighted average. For six VIS/SWIR Landsat bands

$$a_{TOA} = Albedo = \frac{1}{6}\sum_{1}^{6}\rho_\lambda \tag{9}$$

Alternatively the method proposed by Liang (2000)

$$a_{TOA} = \frac{0.356\rho_1 + 0.130\rho_3 + 0.373\rho_4 + 0.085\rho_5 + 0.072\rho_7 - 0.0018}{0.356 + 0.130 + 0.373 + 0.085 + 0.072} \tag{10}$$

uses different weights for different bands. Note that Liang does not use band 2 (the green part of the spectrum).

The band-averaged albedo can be corrected for terrain slopes if one has the total insolation field (from 6) or that given by Solar Analyst (SAT). In this latter case

$$a_{CORR} = a_{TOA}[\frac{S \cdot \cos(\theta_S)}{SAT}] \quad (11)$$

This formula will decrease the albedo estimate for a brightly illuminated hill slope and increase it for a pixel in shadow. This formula can cause problems when the SAT predicts large beam attenuation or if there is large path radiance. Albedo should always lie in the range zero to one.

Using the albedo (e.g. TOA or corrected), we can estimate the absorbed solar radiation for each pixel in the scene.

$$AbsorbedSolar = TotalSolar \cdot (1 - a) \quad (12a)$$

$$AbsorbedSolar = SAT \cdot (1 - a) \quad (12b)$$

depending on which estimate of total insolation is preferred.

3. Thermal Infra-red radiation

a. Upward long wave radiation

The emitted long wave radiation from the earth's surface is given by

$$F_S = \varepsilon_S \sigma T_S^4 \quad (13)$$

Where T_S is the surface temperature, ε_S is the surface emissivity and $\sigma = 5.67 \times 10^{-8} W \cdot m^{-2} \cdot K^{-4}$ is the Stefan-Boltzman Constant. In the TIR part of the spectrum, the emissivity is usually close to unity; say $\varepsilon_S \approx 0.95$. With this value, a surface with temperature of 300K emits with a power of 436W/m2.

b. Downward Long Wave Radiation

The earth's atmosphere also emits long wave radiation, because of the presence of greenhouse gases such as carbon dioxide and water vapor. The downgoing long wave radiation plays a significant role in the surface heat budget. It is estimated from

$$F_A = \varepsilon_A \sigma T_A^4 \quad (14)$$

where T_A is the lower atmosphere temperature and ε_A is the atmospheric emissivity. Several different methods have been proposed to estimate ε_A . Staley and Jurica, (1974) suggested

$$\varepsilon_A = Ce^m \quad (15a)$$

where C=0.67, m=0.08 and "e" is the partial pressure of water vapor in the range $0.2mb < e < 20mb$. As the variation predicted by (15) is rather small, we will use a

single value at sea level: $\varepsilon_A = 0.67$. With this value, an atmospheric temperature of 280K would give $F_A = \varepsilon_A \sigma T_A^4$=233W/m2. Most of this downgoing longwave radiation is absorbed by the earth's surface. To account for reduced longwave radiation with altitude, we suggest

$$\varepsilon_A = Ce^{-z/2H_S} \tag{15b}$$

under the assumption that the emissivity is proportional to the square root of air density. The density scale height is Hs=8000m. At z = 4000meters, the emissivity is reduced from 0.67 to 0.52.

The temperature of the atmosphere varies from day to day, season to season and with altitude. For a first approximation, one could use the U.S. Standard Atmosphere for mid-latitudes

$$T_A(z) = 15 - 6.5 \cdot z \tag{16}$$

where $T_A(z)$ is the air temperature in Celsius and "z" is the altitude in kilometers. For example, the air temperature at z = 5000m is -17.5C = 255.6K. In most cases it will be important to use local meteorological data instead of the Standard Atmosphere. For example, for the Denali image on 27 September 2001, a better formula would be $T_A(z) = 10 - 7.6 \cdot z$ so at z = 5000m the air temperature is -28C = 245K.

For this exercise using Mt Whitney on 20 July 2000, we use $T_A(z) = 35 - 8 \cdot z$ so the temperature at z = 5000m is -5C=268K.

c. Net Radiation

Using these long wave estimates, we can compute the net radiation received by the surface including short and long waves.

$$R_N = AbsorbedSolar - F_S + F_A$$

or

$$R_N = SAT(1-a) - \varepsilon_S \sigma T_S^4 + \varepsilon_A \sigma T_A^4 \tag{17}$$

4. Turbulent Heat transfer between the earth's surface and the atmosphere

a. Sensible heat

A substantial fraction of heat received by the earth's surface from the sun is transported quickly to the atmosphere by conduction, convection and evaporation (FT). Estimates of these heat fluxes are always uncertain as they depend on a number of variables such as wind speed, surface roughness, atmospheric stability and surface wetness. With a fully instrumented meteorological tower, the fluxes can be measured using the eddy-covariance method. Without this data, we must estimate the heat fluxes using an empirical exchange equation. For sensible heat

$$H = \rho C_P C_{DH} U (T_S - T_A) \tag{18}$$

with air density $\rho \approx 1.2 kg/m3$ at sea level and specific heat capacity $C_P = 1004 J/kg \cdot K$ (Hartmann, 1994, page 101) The exchange coefficient (C_{DH}) depends on the wind speed, surface roughness and on $\Delta T = (T_S - T_A)$ itself. If the wind speed U=5m/s and the exchange coefficient $C_{DH} = 0.003$, (13) becomes

$$H \approx 15(T_S - T_A) \tag{19}$$

so a one degree temperature difference between the surface and the air would produce a heat flux of 15W/m2. When the surface is colder than the air (i.e. stable conditions), the turbulence is weaker and the value of C_{DH} is smaller. This uncertainty will be a source of error in our calculations.

b. Latent Heat

When the surface is moist (e.g. forest and water surfaces) evapo-transpiration plays a large role in the heat budget. The heat of evaporation is carried upwards in the turbulent flux of water vapor; so called latent heat flux. As a global average, the rate of evaporation (ER) is given approximately by

$$ER(mm/month) \approx 5 \cdot T_S(°C) \tag{20}$$

if the temperature exceeds zero Celsius and ER=0 otherwise. On a per second basis, this is

$$ER(mm/s) \approx (1.85 \times 10^{-6}) \cdot T_S(°C) \tag{21}$$

Using the latent heat of evaporation of water ($L_W = 2.5 \cdot 10^6 J/kg$) and the density of liquid water ($\rho_W = 1000 kg \cdot m^{-3}$), the daily average latent heat flux (from 21) is

$$L = 4.6 \cdot T_S(°C) \tag{22}$$

For example, if water is available, an average surface temperature of 10C will give 46W/m2 of latent heat transport. During the day, the value could be double the daily average value. For the purposes of this exercise, we recommend that the cooling by evapo-transpiration be estimated from

$$L = 10 \cdot T_S(°C) \tag{23}$$

when $T_S > 0°C$ for dense vegetation. For variable vegetation density, we scale the latent heat with NDVI, so

$$L = 10 \cdot [\frac{NDVI - 0.2}{0.6}] \cdot T_S(^\circ C) \quad (24)$$

for $NDVI > 0.2$. Otherwise, L = 0. For example, if NDVI = 0.5 and the surface temperature is 10C, the latent heat flux will be 50W/m2. The uncertainty in this formulation will be a source of error in our calculations.

Another approach is to use the Bowen Ratio $\beta = H / L$. If the Bowen Ratio and sensible heat are known for each pixel, the latent heat is $L = H / \beta$. The Bowen Ratio varies with the nature and water availability of the surface. For forested areas, $\beta < 0.5$ while for dry grasslands, $\beta > 2$. For a trial, one could try to estimate the Bowen ratio from NDVI.

c. Total turbulent heat flux

The total turbulent heat flux is the sum of the sensible and latent heat fluxes

$$F_T = H + L \quad (25)$$

5. Estimating the surface heat imbalance

A spatial analysis of heat budget requires several layers describing the land cover (e.g. elevation, NDVI, NDSI,, etc.) and several layers describing factors or terms in the heat budget equation (e.g. absorbed solar, net radiation, sensible and latent heat, etc). A useful additional diagnostic quantity is

$$imbalance = R_N - F_T \quad (26)$$

This quantity is equivalent to the storage term in (0) but we interpret it more broadly. A non-zero value of "imbalance" could be

1. heat storage, as in (0)
2. melting ice, absorbing heat as ice is converted to liquid
3. errors in R_N or F_T

By comparing the spatial pattern of heat budget terms with the land cover distribution, it may be possible characterize each land cover type by its heat budget.

6. Other applications of the heat budget equation

The methods above are intended to be used in the optional lab 11 exercise for OEFS. For students wishing to go further, some additional exercises are listed below.

1. Have ERMapper perform statistics on the full stack. Discuss the correlations between layers.

2. Is the effect of vegetation on heat budget largely evaporation, or is surface roughness an equally important factor?
3. If your calculation shows a large positive heat flux to a lake or snow field, compute the rate of evaporation or melting.
4. Try to improve the balance between estimated net radiation and turbulent heat flux in your study area by improving one or more of the parameterizations.
5. Using your own Total insolation field, or that from Solar Analyst (SAT), design ways to correct albedo values for atmospheric and terrain slope effects.
6. Compare two small areas near campus, using the portable spectrometer and portable IR thermometer instead of satellite data. Use a Kestrel for air temperature and wind speed. For example, compare a grass and pavement area in mid day or at night. Off campus, compare a cornfield and a plowed field.
7. Repeat the exercise using a Landsat image with a different selection of land cover types: forest, agriculture fields, barren, snow, water, or latitude. ASTER or MODIS could be used instead.
8. Repeat the exercise with a Landsat image of a large city, such as St. Louis, Beijing, Paris, Santiago, etc.
9. Use a sequence MODIS images to study a larger region over time. Deduce the seasonal cycle of the heat budget.
10. Use a sequence of MODIS images from a region with recent climate change to see how the heat budget responds to heat waves or drought.
11. Classify the results of a heat budget analysis to identify the different types of surface heat budget in the image.
12. Compare your heat budget results at a point with online data sets from flux-tower reference sites (Ameriflux, ARM, T-REX) or gridded North America Regional Re-analysis (NARR) data. How do the heat flux terms in these datasets vary during the day and with season? Are your results representative?

7. Global Heat Budget Diagram

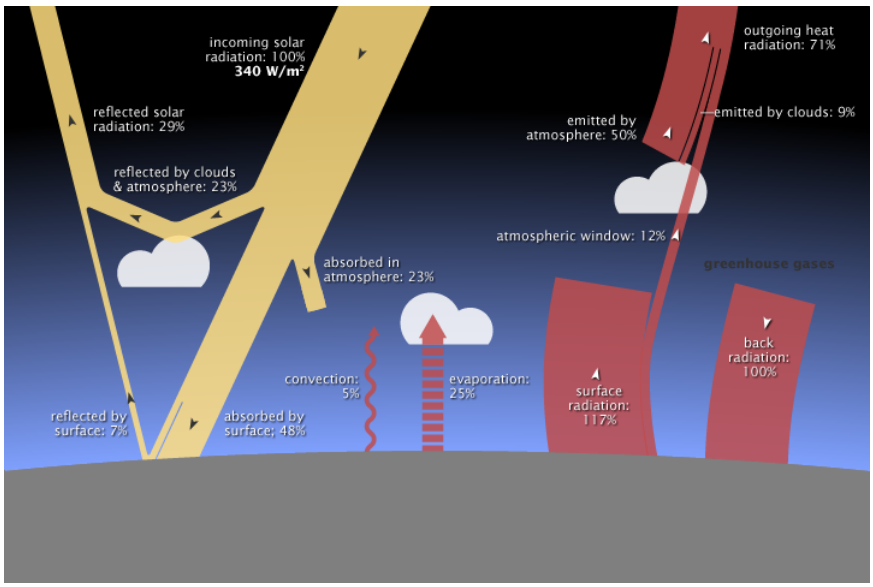

This diagram (from NASA) shows the components of the earth's heat budget. The components active at the surface are the subject of this lab exercise.

8. References

Barry, Roger G., 1992, Mountain weather and climate, 2nd Edition, Routledge, 402p

Hartmann, D. L., 1994, Global Physical Climatology, Academic press, 411p

Liou, K.N., 2002, An introduction to Atmospheric radiation, Academic press, 583p

Stull, R.B., 2004, "An introduction to Boundary Layer Meteorology" , Springer, 680p

The Role of Rural Variability in Urban Heat Island Determination for Phoenix, Arizona Timothy W. Hawkins, Anthony J. Brazel, William L. Stefanov, Wendy Bigler, and Erinanne M. Saffell *Journal of Applied Meteorology*
Volume 43, Issue 3 (April 2004) pp. 476–486

Urban Modification of the Surface Energy Balance in the West African Sahel: Ouagadougou, Burkina Faso B. Offerle, P. Jonsson, I. Eliasson, and C. S. B. Grimmond *Journal of Climate* Volume 18, Issue 19 (October 2005) pp. 3983–3995

Comparing Temperature and Humidity on a Mountain Slope and in the Free Air Nearby Morris H. McCutchan *Monthly Weather Review* ,Volume 111, Issue 4 (April 1983) pp. 836–845

Variation in Surface Energetics during Snowmelt in a Subarctic Mountain Catchment J. W. Pomeroy, B. Toth, R. J. Granger, N. R. Hedstrom, and R. L. H. Essery *Journal of Hydrometeorology* ,Volume 4, Issue 4 (August 2003) pp. 702–719

Effect of Elevation and Aspect on Wind, Temperature and Humidity Morris H. McCutchan and Douglas G. Fox *Journal of Applied Meteorology*
Volume 25, Issue 12 (December 1986) pp. 1996–2013

Effects of Slope and Aspect Variations on Satellite Surface Temperature Retrievals and Mesoscale Analysis in Mountainous Terrain Alan E. Lipton *Journal of Applied Meteorology* ,Volume 31, Issue 3 (March 1992) pp. 255–264

The Influence of Land Use/Land Cover on Climatological Values of the Diurnal Temperature Range Kevin P. Gallo, David R. Easterling, and Thomas C. Peterson *Journal of Climate* ,Volume 9, Issue 11 (November 1996) pp. 2941–2944

Zaitchik, BF; Macalady, AK; Bonneau, LR; Smith, RB. 2006. Europe's 2003 heat wave: a satellite view of impacts and land-atmosphere feedbacks. *International Journal of Climatology* 26 (6): 743-769.

Liang, S. 2000. "Narrowband to broadband conversions of land surface albedo I algorithms." *Remote Sensing of Environment* 76, 213-238.

Law, H.K. and Nichol, L. 2004. "Topographic Correction for Differential Illumination Effects on Ikonos Satellite Imagery." *International Archives of Photogrammetry Remote Sensing and Spatial Information Sciences* 35, 641-646.

Schneider, C., E. Parlow. D., Scherer, 1996, GIS-based modeling of the energy balance of Tarfala Valley, Sweden using Landsat-TM data, Progress in Remote sensing research and Applications. ISBN 90 5410 5984